

Characterization of Lithium-ion Cathode Material Using Artificial Neural Network

Okonkwo F.C, Onochojah U, Ichu B. C and Uwakwe E.

Lithium-ion Battery Research Group, Projects Development Institute (PRODA), P.M.B. 01609, Emene, Enugu, Nigeria

Corresponding Author; Okonkwo F.C

ABSTRACT

Cathode active materials are the main elements dictating the differences in the composition of battery cells. The cathode materials comprised of cobalt, nickel and manganese in the crystal structure forming a multi-metal oxide material to which lithium is added. Artificial neural network was proposed for the characterization of lithium ion cathode material to determine the existence of x-ray diffraction peaks at different degrees and layered structure of the sample. The model was classified for training, testing and validation. The data obtained from the synthesized cathode materials ($\text{LiNi}_{0.5}\text{Mn}_{0.5}\text{O}_2$) were used as inputs and processed as x-ray diffraction patterns. The design and analysis was done with MATLAB/SIMULINK software. The results obtained gave 82.97% accuracy of x-ray diffraction pattern prediction for cathode materials.

DATE OF SUBMISSION: 15-01-2020

DATE OF ACCEPTANCE: 31-01-2020

I. INTRODUCTION

Considering various technologies for storing energy, the usage of lithium (Li) – ion batteries still stands as one of the most promising options, especially for the on-going huge demand for electric and plug-in hybrid vehicles. The main limiting factor in the performance of a Li-ion battery is the cathode material and design specifications.

Lithium-ion batteries comprise of the anode, cathode, separator and the supporting solution in which progression of lithium ions from the cathode to anode and vice versa during charge/discharge process [1]. The materials that are typically used for fabricating the anode are metallic lithium, graphitic carbon, hard carbon, synthetic graphite, lithium titanate; tin-based alloys and silicon-based materials [2]. The materials used for making cathode are an oxide of lithium manganese, lithium cobalt oxide, FeS_2 , V_2O_5 , lithium nickel cobalt manganese oxide, lithium ion phosphate and electronic conducting polymers [3]. The materials used as electrolytes include LiPF_6 , LiClO_4 , LiAsF_6 and LiCF_3SO_3 [4]. Apart from these main components, there are other components such as a binder, flame retardant, gel precursor and electrolyte solvent [5].

Battery design based on experiments is time-consuming and expensive. In contrast, simulation-based design is not only more efficient, but also provides deeper insights into the mechanisms governing the battery performance [6]. The majority of current battery models are based

on the pseudo two-dimensional (P2D) electrochemical model, which is based on the porous electrode theory [3]. The P2D model has been used to optimize the cathode and anode thickness, porosity, particle size and many other important electrode parameters.

High-throughput material synthesis and rapid characterization are necessary ingredients for design and accelerated material discovery [7]. X-ray diffraction (XRD) is a workhorse technique to determine crystallography and phase information, including lattice parameters, crystal symmetry, phase composition, density, space-group, and dimensionality [7]. This technique works on the principle of Bragg's law, where the material is bombarded with X-rays at different angles and the intensity of the beam is measured. This is achieved by mapping XRD patterns for a material to the measured or simulated XRD patterns of known materials [8].

Despite its indispensable utility, XRD is a common bottleneck in materials-characterization loops; up to one hour is typically required for thin-film XRD data acquisition for a 2θ scan with high angular resolution, and another one to two hours are typically required for Rietveld refinement by an expert crystallographer when the crystalline phases are known. It is widely recognized that machine learning methods have potential to accelerate this process; however, practical implementations have thus far focused on well-established materials, require combinatorial datasets spanning among various phases or require large datasets [9]. In this

study, artificial neural network technique will be applied to the characterization of lithium ion cathode material ($\text{LiNi}_{0.5}\text{Mn}_{0.5}\text{O}_2$) and also compare the percentage accuracy of the model developed.

II. ELECTRODE MATERIALS

2.1 Cathode Materials

Over the last two decades there has been intensive research in improving the overall performance of Li - ion batteries. Among the different components of the battery mechanism one of the main attention has been alternative cathode materials. Cathode materials can primarily be categorized based on structure types; LiCoO_2 , LiNiO_2 , Li_2MnO_3 , $\text{LiNi}_{1-x}\text{Co}_x\text{O}_2$, $\text{LiNi}_{1/3}\text{Mn}_{1/3}\text{Co}_{1/3}\text{O}_2$ etc.

2.1.1 Layered Structure Metal Oxides

These materials usually have layered $\alpha\text{-NaFeO}_2$ structure, which is a distorted rock-salt structure where the cations order in alternating (1 1 1) planes [10]. This ordering results in a triangular structure also known as R3m space group. In these structures the oxygen atoms are arranged in a face centered cubic close-packed arrangement with the transition metal oxides present within the oxygen octahedral and the lithium atoms would reside in the space between the oxygen layers. This structure supports the intercalation process where the lithium ions are inserted and removed from the structures during charge and discharge cycles as depicted in figure 1[11].

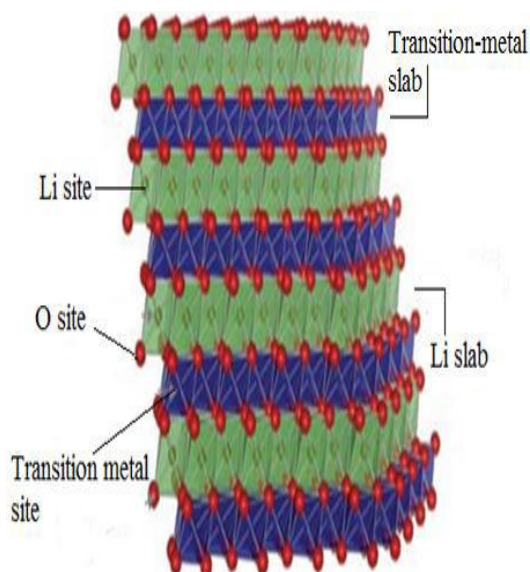


Figure 1: Layered structured transition metal oxides.

2.1.2 LiCoO_2

Presently the lithium ion battery industry is dominated by the LiCoO_2 cathodes and carbon anodes first introduced by Sony in 1991. This

material was first reported by John Goodenough who recognized that this material had layered structure and that lithium could be removed electrochemically, thus making it a promising cathode material.

LiCoO_2 has $\alpha\text{-NaFeO}_2$ structure with O atoms present in a cubic closely-packed face-centered cubic (FCC) arrangement, when lithium is completely removed; the oxygen layers rearrange themselves to give hexagonal close packing in form of CoO_2 . Figure 2 represents the layered structure of LiCoO_2 [11].

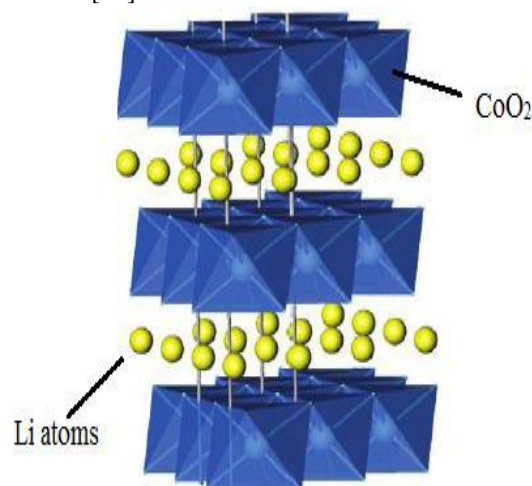


Figure 2: Layered structure of LiCoO_2 [11].

Though LiCoO_2 cathode material is leading the lithium-ion battery market, there is limited availability of cobalt, thereby making it an expensive material. A lot of research is being done to find a probable replacement for Co with materials that are abundant and that are environmental friendly such as Ni, Mn, Fe and Cr.

2.1.3 $\text{LiNi}_{1-y}\text{Mn}_y\text{O}_2$

Lithium nickel manganese oxides have been of great interest among researchers for advanced lithium-ion batteries and as a possible replacement for LiCoO_2 . Figure 3, shows a unit cell of $\text{LiMn}_y\text{Ni}_{1-y}\text{O}_2$.

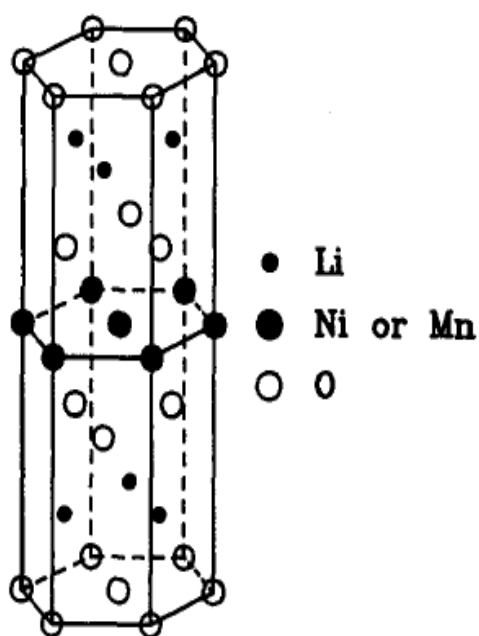


Figure 3: Unit cell of $\text{LiMnyNi}_{1-y}\text{O}_2$ showing Li-filled and Ni, Mn-filled layers [12].

The main advantage of this material is that there is no CO content which is very expensive and a toxic compound compared to Ni and Mn. The most

successful material of this group has been $\text{LiNi}_{1/2}\text{Mn}_{1/2}\text{O}_2$

2.1.4 LiMnO_2 (layered)/ LiMn_2O_4 (spinel)

Along with its counterparts such as LiNiO_2 and LiCoO_2 , this material has also been researched a lot over the last decade mainly for its prospects of providing not only a low-cost but also an environmentally benign cathode material [13]. In spite of these advantages LiMnO_2 was never a viable cathode mainly because this material is unstable at elevated temperatures and cannot be synthesized by the same methods as used for materials like NaMnO_2 .

When LiMnO_2 is synthesized, it tends to revert itself to form a more stable spinel structure LiMn_2O_4 . LiMn_2O_4 has proven to be a viable cathode material mainly because of the three dimensional framework which adds stability to the structure during delithiation. Additionally, unlike LiNiO_2 and LiCoO_2 , this material does not react exothermically with the electrolyte making it potentially safer than LiNiO_2 and LiCoO_2 . Figure 4 shows a comparison between LiMnO_2 and LiMn_2O_4 structures. The tunnel like structure for LiMn_2O_4 allows lithium to move out of the structure without collapse even under high charge/discharge rates.

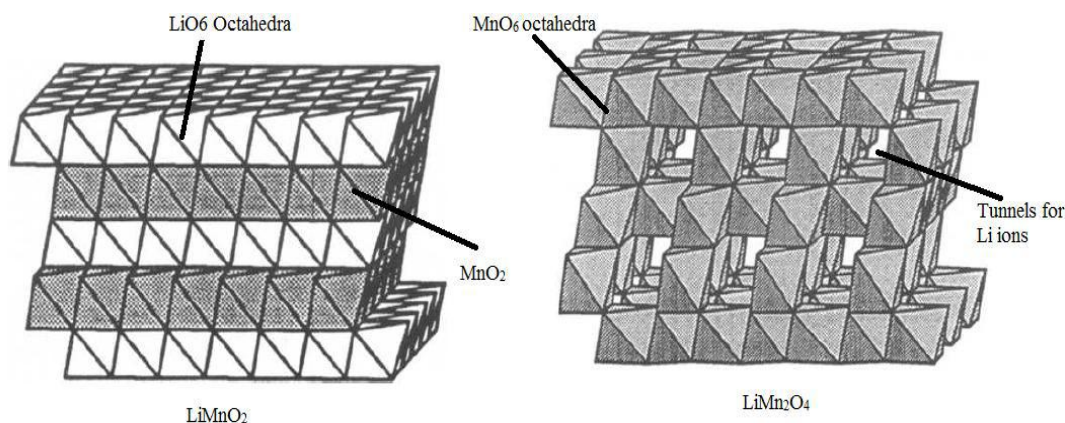


Figure 4: Comparison between layered LiMnO_2 structure and Spinel LiMn_2O_4 structure [13].

2.2 Anode materials

Anode materials are necessary in Li-ion batteries because Li metal forms dendrites which can cause short circuiting, start a thermal run-away reaction on the cathode, and also causes the battery to catch fire. Li metal also suffers from poor cycle life.

2.2.1 Graphitic and hard carbons

Electrochemical activity in carbon comes from the intercalation of Li between the graphene planes, which offer good 2D mechanical stability, electrical conductivity, and Li transport and Li

transport. Carbon has the combined properties of low cost, abundant availability, low delithiation potential vs Li, high Li diffusivity, high electrical conductivity, and relatively low volume change during lithiation/ delithiation as shown in Table 1. Thus carbon has an attractive balance of relatively low cost, abundance, moderate energy density, power density, and cycle life, compared to any other intercalation-type anode materials. Carbon's gravimetric capacity is higher than most cathode materials but the volumetric capacity of commercial graphite electrodes is still small ($330\text{--}430 \text{ mAh cm}^{-3}$).

Table 1

Properties of some commonly studied anode materials.				
Material	Lithiation potential (V)	Delithiation potential (V)	D (cm ² s ⁻¹)	Volume change
Graphite [182,193–198]	0.07, 0.10, 0.19	0.1, 0.14, 0.23	10 ⁻¹¹ –10 ⁻⁷	10%
LTO [199–203]	1.55	1.58	10 ⁻¹² –10 ⁻¹¹	0.20%
Si [34,191,204–209]	0.05, 0.21	0.31, 0.47	10 ⁻¹³ –10 ⁻¹¹	270%
Ge [34,209–212]	0.2, 0.3, 0.5	0.5, 0.62	10 ⁻¹² –10 ⁻¹⁰	240%
Sn [34,209,213–215]	0.4, 0.57, 0.69	0.58, 0.7, 0.78	10 ⁻¹⁶ –10 ⁻¹³	255%
Li ₂ O [216] (amorphous)	N/A	N/A	5 × 10 ⁻¹² –5 × 10 ⁻¹⁰	N/A

III. METHODOLOGY

The purpose of this work is to develop an artificial neural network model that can characterize a lithium ion cathode materials using data obtained from x-ray diffraction equipment. The first step in constructing a neural network is to determine the inputs and outputs. The inputs are determined from the cathode material synthesized. The synthesis is done by using a sol- gel method or any other methods to obtain a processed cathode material, the concentration, diffusion coefficient,

particle radius, Bruggeman constant, thickness and solid phase volume fraction are chosen as the input variables.

The output of the neural network is obtained by extracting data from the x-ray diffraction set up for a particular sample material which will be used to train the networks in other to make accurate predictions of outputs characterization. Figure 5 represents the SIMULINK model of the design.

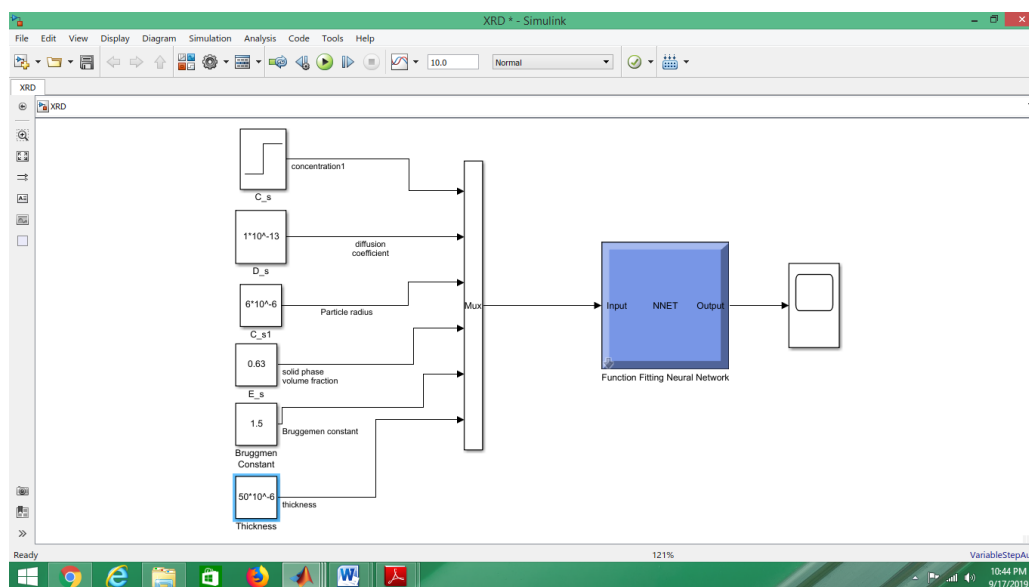


Figure 5: artificial neural network model for characterization of lithium ion () material.

Data of the XRD spectrum of the LiNi_{0.5}Mn_{0.5}O₂ material prepared by sol-gel method at 800 °C for 20 hours was obtained [14] and classified for training testing and validation. The XRD spectrum was indexed based on the α-NaFeO₂ structure with a space group R $\bar{3}$ m [15].

The model for the characterization of LiNi_{0.5}Mn_{0.5}O₂ was created using a Levenberg-Marquardt algorithm. Figure 5 shows the input layer, hidden layer, output layer and output.

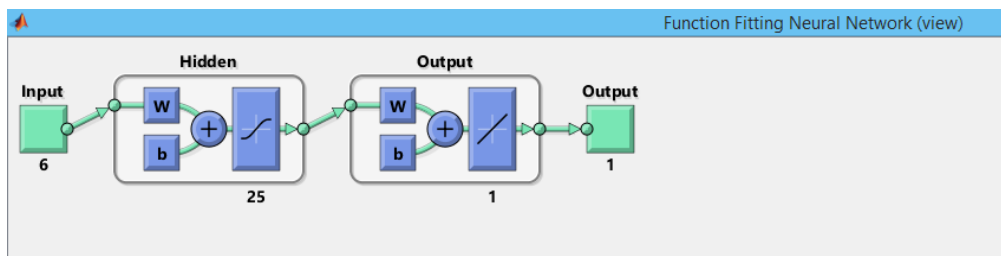


Figure 5: Schematic of neural network layers.

IV. RESULTS AND DISCUSSION

The parameters for $\text{LiNi}_{0.5}\text{Mn}_{0.5}\text{O}_2$ of the synthesized compound used for the simulation is shown in Table 2.

Table 2: Design variables

Variable	Value	Symbol(Unit)
Electrode concentration	25.8×10^{-3}	(molm^{-3})
Active material particle radius	6×10^{-6}	m
solid phase volume fraction	0.6	
Thickness	50×10^{-6}	m
Bruggeman constant	1.5	
Diffusion Coefficient	1×10^{-13}	

A regression plot for the characterization was created as seen in figure 6; it shows the relationship between the output of the network and the targets which typically are represented by a regression factor (correlation Coefficient R). The four plots represent the training, testing data, validation and overall performance of the $\text{LiNi}_{0.5}\text{Mn}_{0.5}\text{O}_2$ characterization. The dashed line in each plot represents the perfect result – outputs = targets. The solid line represents the best fit linear regression line between outputs and targets. The training data indicates a good fit with an R value of 0.92313. The validation and test results also show R values of 0.85267 and 0.91489. The overall model show performance training accuracy 0.91981(91.98%) which indicates that the neural network was well characterize.

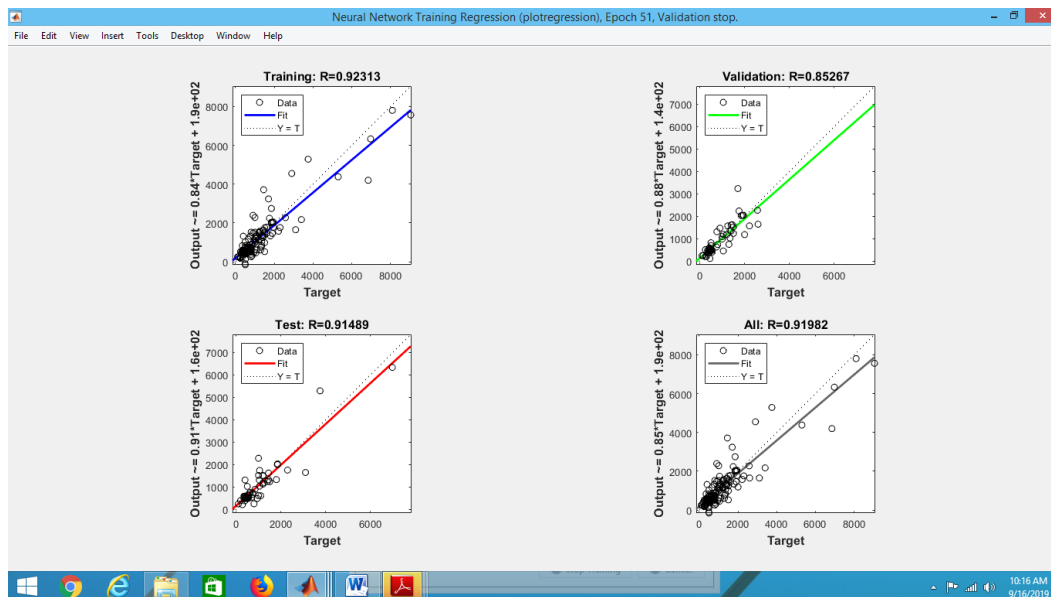


Figure6: Neural network Regression plot

2.3 XRD analysis

Figure 7 represent the XRD pattern of $\text{LiNi}_{0.5}\text{Mn}_{0.5}\text{O}_2$ characterization and the simulated result for $\text{LiNi}_{0.5}\text{Mn}_{0.5}\text{O}_2$ characterization. The experimental set up was used to determine the

existence of doublet XRD peaks at different degrees and layered structure of the sample [15]. The result obtained shows a close relation between the XRD experimental pattern and the artificial neural network model.

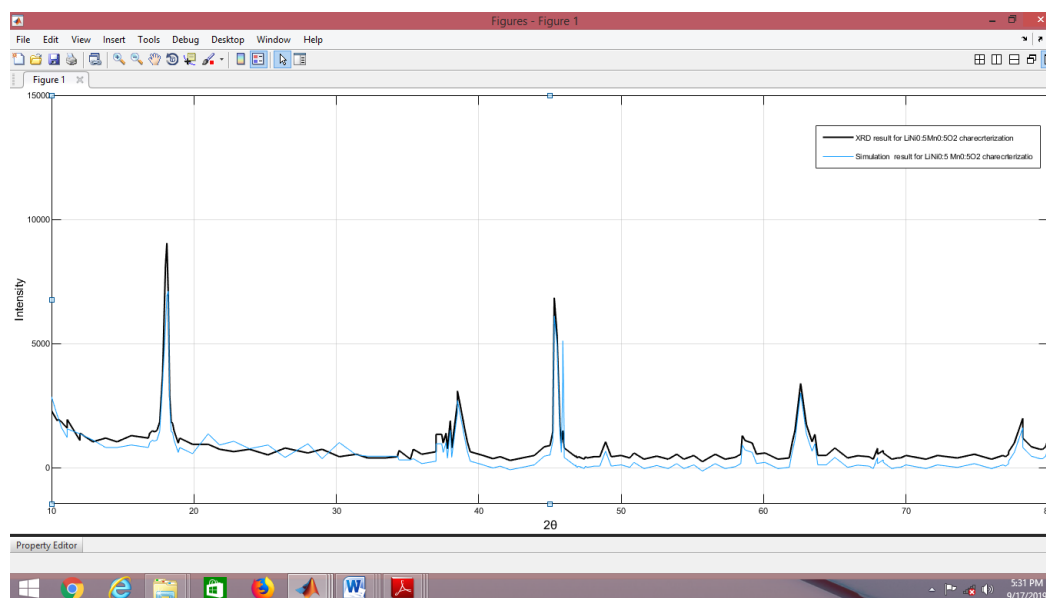


Figure 7: Comparison of XRD pattern and ANN model for $\text{LiNi}_{0.5}\text{Mn}_{0.5}\text{O}_2$.

The graph shows a relationship between intensity (number of counts) to diffraction angles (2θ). The XRD gave a maximum peak at 9051 counts at 18.1° while the ANN model recorded a

maximum peak at 7121 counts at 18.2° . The proposed model indicates a close relationship with the experimental result and has a percentage accuracy of 82.97% as express below.

$$\text{XRD} = \frac{\sum 9051 + 3101 + 6851 + 1051 + 1301 + 3401 + 2000}{7} = 3822.3$$

$$\text{ANN} = \frac{\sum 7121 + 2722 + 6121 + 671.9 + 921.9 + 3022 + 1621}{7} = 3171.5$$

$$\text{Percentage error} = \frac{3822.3 - 3171.5}{3822.3} * 100 = 17.03\%$$

The percentage error is 17.03%.

$$\text{Percentage accuracy} = 100 - 17.03 = 82.97\%$$

V. CONCLUSION

In this work an artificial neural network model was designed for the characterization of lithium ion battery electrode material. The data used was gotten from x-ray diffraction set up and the synthesis of $\text{LiNi}_{0.5}\text{Mn}_{0.5}\text{O}_2$ material using sol-gel method at 800°C for 20 hours. The model was classified for training testing and validation using the data obtained. The neural network was used to predict the characterization pattern of lithium ion cathode material to determine if a set of input variables is physically feasible. Comparison between the artificial neural network and the experimental result gave a satisfactory accuracy. The proposed model provides a framework for creating more efficient models for lithium ion battery characterization.

REFERENCE

- [1]. M.A. Hannan, M.M. Hoque, A. Hussain, Y. Yusof, P.J. Ker, State-of-the-art and energy management system of lithium-ion batteries in electric vehicle applications: issues and recommendations, IEEE (2018) 19362–19378.
- [2]. A. Mishra, A. Mehta, S. Basu, materials - science - for - energy-technologies, Electrode materials for lithium-ion batteries 1 (2018) 182–187
- [3]. Bin Wua, Sangwoo Hana, Kang G. Shinb, Wei Lua,*Application of artificial neural networks in design of lithium-ion batteries, Journal of Power Sources 2018.
- [4]. D. A. Carr, M. Lach-hab, S. Yang, I. I. Vaisman, and E. Blaisten-Barojas, “Machine learning approach for structure-based zeolite classification,” Microporous/Mesoporous Mater., vol. 117, no. 1–2, pp. 339–349, 2009.
- [5]. G.A. Elia, J.B. Park, Y.K. Sun, B. Scrosati, J. Hassoun, Role of the lithium salt in the performance of lithium-oxygen batteries: a comparative study, ChemElectroChem 1 (2014) 47–50.
- [6]. N.S. Xue, W.B. Du, A. Gupta, W. Shyy, A.M. Sastry, J.R.R.A. Martins, J. Electrochem. Soc. 160 (2013) A1071–A1078.
- [7]. A. Tabor, D. Roch, and L. Saikin, “Lawrence Berkeley National Laboratory Recent Work Title Accelerating the discovery of materials for clean energy in the era of smart automation Publication Date, 2018.
- [8]. D. A. Carr, M. Lach-hab, S. Yang, I. I. Vaisman, and E. Blaisten-Barojas, Machine learning approach for structure-based zeolite classification, Microporous/Mesoporous Mater., vol. 117, no. 1–2, pp. 339–349, 2009.

- [9]. W. B. Park et al., "Classification of crystal structure using a convolutional neural network," IUCrJ, vol. 4, pp. 486–494, 2017.
- [10]. Shaju, K.M., G.V. SubbaRao, and B.V.R. Chowdari, Performance of layered $\text{Li}(\text{Ni}_{1/3}\text{Co}_{1/3}\text{Mn}_{1/3})\text{O}_2$ as cathode for Li-ion batteries. *ElectrochimicaActa*, 2002. 48(2): p. 145-151.
- [11]. M.Armand, J.M.T.a., Issue and challenges facing rechargeable lithium batteries. *Nature*, 2001. 414(6861): p. 359-367
- [12]. Akimoto, J., Y. Gotoh, and Y. Oosawa, Synthesis and Structure Refinement of LiCoO_2 Single Crystals. *Journal of Solid State Chemistry*, 1998. 141(1): p. 298-302.
- [13]. E. Michael, S. Bernhard, O. Haas^s and R. Nesper, Characterization of Layered Lithium Nickel Manganese Oxides Synthesized by a Novel Oxidative Coprecipitation Method and Their Electrochemical Performance as Lithium Insertion Electrode Materials. *Journal of the Electrochemical Society*, 1998. 145(4): p. 1113-1121.
- [14]. A.R. Armstrong, and P.G. Bruce, Synthesis of layered LiMnO_2 as an electrode for rechargeable lithium batteries. *Nature*, 1996. 381(6582): p. 499-500.
- [15]. N. Murali, k. Vijaya, k. Ephraim, V. Veeraiyah, Structural and conductivity studies of $\text{LiNi}_{0.5}\text{Mn}_{0.5}\text{O}_2$ cathode., *Materials Science-Poland*, 34(2), 2016, pp. 404-411.
- [16]. C.P.Grey, W.S.Yoon, J. reed, G.ceder, *Electrochem.Solid State Lett.*, 7 (2004), A290.

Okonkwo F.C, et.al "Characterization of Lithium-ion Cathode Material Using Artificial Neural Network " *International Journal of Engineering Research and Applications (IJERA)*, vol.10 (01), 2020, pp 34-40.